Acta Crystallographica Section F
Structural Biology and Crystallization Communications
ISSN 1744-3091

Purification, crystallization and preliminary crystallographic characterization of the caspase-recruitment domain of human Nod1

Thiagarajan Srimathi,[a] Sheila L. Robbins,[a] Rachel L. Dubas,[a] Jang-Hoon Seo[b] and Young Chul Park[a]*

[a]Basic Science, Fox Chase Cancer Center, Philadelphia, PA 19111, USA, and [b]Department of Clinical Laboratory Science, Shinheung College, Uijeongbu, Kyungki-Do 480-701, South Korea

Correspondence e-mail: young.park@fccc.edu

Received 26 September 2006
Accepted 1 December 2006

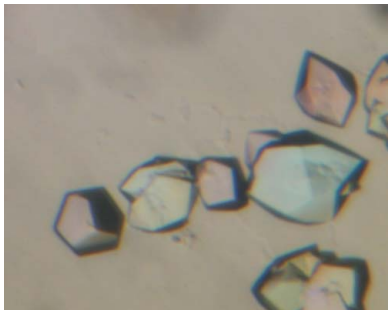

The caspase-recruitment domain (CARD) is known to play an important role in apoptosis and inflammation as an essential protein–protein interaction domain. The CARD of the cytosolic pathogen receptor Nod1 was overexpressed in *Escherichia coli* and purified by affinity chromatography and gel filtration. The purified CARD was crystallized at 277 K using the microseeding method. X-ray diffraction data were collected to 1.9 Å resolution. The crystals belong to space group $P3_1$ or $P3_2$, with unit-cell parameters $a = b = 79.1$, $c = 80.9$ Å. Preliminary analysis indicates that there is one dimeric CARD molecule in the asymmetric unit.

1. Introduction

Nod1 plays an important role in innate immunity as a cytoplasmic sensor of microbial components derived from cell-wall peptidoglycan (PGN; Girardin *et al.*, 2003). Recently, it has also been shown that polymorphisms of the Nod1 gene are associated with inflammatory bowel disease (McGovern *et al.*, 2005) and asthma (Hysi *et al.*, 2005). In addition, Nod1 is also involved in host defense against *Helicobacter pylori* infection, which can cause peptic ulcers and gastric cancer (Viala *et al.*, 2004). The Nod1 molecule consists of three domains. The C-terminal leucine-rich repeat (LRR) domain is responsible for the recognition of bacterial PGN. The middle nucleotide-binding and oligomerization domain (NOD) facilitates self-oligomerization of Nod1, while the N-terminal caspase-recruitment domain (CARD) interacts with other downstream signaling proteins that also possess CARD modules [including, for example, receptor-interacting protein 2 (RIP2) and caspase-1]. The recognition of bacterial PGN initiates the oligomerization-driven activation process of Nod1. Subsequently, activated Nod1 can recruit RIP2 or caspase-1 through the homotypic CARD–CARD interaction. The interaction of Nod1 with RIP2 activates a transcription factor NF-κB and induces the expression of genes involved in immune response (Inohara *et al.*, 2000). Nod1 interaction with caspase-1 leads to the production of IL-1β (Yoo *et al.*, 2002). However, the molecular mechanisms through which Nod1 activates the innate immune response are not fully understood.

The 80-amino-acid CARD possesses a death-domain fold which is formed by six α-helices (Weber & Vincenz, 2001). Like other members of the death-domain superfamily, such as the death domain, the death-effector domain and the pyrin domain, CARD mediates homotypic interactions in which the CARD of one protein interacts with a similar CARD module of another protein. Since many CARD-containing proteins have been identified as important players in the innate immune response, structural and functional insight into the CARD–CARD interaction is critical to understand the molecular mechanisms of this initial immune response.

Crystal structures of the monomeric CARDs of Apaf-1 (Vaughn *et al.*, 1999) and caspase-9 (Qin *et al.*, 1999) and NMR structures of the monomeric CARDs of RAIDD (Chou *et al.*, 1998) and ICEBERG (Humke *et al.*, 2000) are available in the PDB and only one crystal structure of a heterodimeric complex (Apaf-1 and caspase-9) has been determined (Qin *et al.*, 1999). However, no crystal structures of a CARD directly involved in pathogen recognition are available

Table 1
Data-processing statistics for the native data set measured at MacCHESS F2.

Wavelength (Å)	0.977
Temperature (K)	100
Resolution	50.0–1.82 (1.96–1.89)
Measured reflections	276184
Unique reflections	26612
Redundancy	5.5 (3.4)
Space group	$P3_1$ or $P3_2$
Unit-cell parameters (Å)	$a = b = 79.1$, $c = 80.9$
Completeness (%)	99.6 (96.5)
Mean $I/\sigma(I)$	29.2 (4.58)
R_{sym}†	0.076 (0.49)

† $R_{sym} = \sum_{\mathbf{h}} \sum_l |I_{\mathbf{h}l} - \langle I_{\mathbf{h}} \rangle| / \sum_{\mathbf{h}} \sum_l \langle I_{\mathbf{h}} \rangle$, where I_l is the lth observation of reflection **h** and $\langle I_{\mathbf{h}} \rangle$ is the weighted average intensity for all observations l of reflection **h**.

owing to difficulties in purification and crystallization. In order to provide further structural insight into the CARD–CARD interaction involved in the innate immune response, the Met1–Glu106 caspase-recruitment module of human Nod1 (Nod1_CARD; ∼13 kDa molecular weight) was purified and crystallized.

2. Materials and methods

2.1. Cloning, expression and purification

The coding region of CARD, Met1–Glu106, was amplified by PCR using human Nod1 cDNA (GenBank accession No. BC040330) as the template and cloned into pET24d (Novagen), adding a C-terminal hexa-His tag to the expressed protein. *Escherichia coli* Rosetta-pLysS cells were used to express the recombinant protein. Cells were grown in LB medium with 0.5%(*w*/*v*) glucose to an OD_{600} of 0.6. Protein expression was then induced by adding 1 m*M* IPTG at 310 K and maintained for 3 h. The culture was harvested by centrifugation for 15 min at 8000*g* and 277 K. Harvested cells were resuspended in lysis buffer [50 m*M* sodium phosphate pH 7.0, 1.5 *M* NaCl, 1.5 *M* urea, 10%(*v*/*v*) glycerol, 3 m*M* β-mercaptoethanol] and then sonicated. The lysate was cleared by centrifugation for 30 min at 38 000*g* and 277 K. Cleared cell extract was incubated with Ni resin (Qiagen) which had been pre-equilibrated with lysis buffer. The resin was washed with wash buffer [50 m*M* sodium phosphate pH 6.0, 300 m*M* NaCl, 10%(*v*/*v*) glycerol, 20 m*M* imidazole, 3 m*M* β-mercaptoethanol] and transferred onto the column. The protein was eluted from the resin with elution buffer [50 m*M* sodium phosphate pH 6.0, 300 m*M* NaCl, 10%(*v*/*v*) glycerol, 300 m*M* imidazole, 3 m*M* β-mercaptoethanol]. The fractions containing Nod1_CARD were combined and concentrated using a 10.0 kDa cutoff filter (Millipore). The concentrated Nod1_CARD was further purified using a Superdex-75 gel-filtration column (Amersham Bioscience) in 10 m*M* sodium phosphate pH 6.0, 130 m*M* NaCl, 1 m*M* DTT. The concentration of purified Nod1_CARD was determined using a Bicinchoninic Acid kit (Sigma) and the purity was determined by SDS–PAGE.

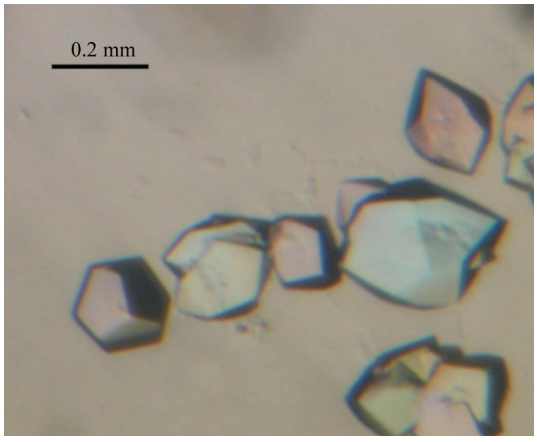

Figure 1
Crystals of CARD (Met1–Glu106) of Nod1.

2.2. Crystallization

The initial screening of crystallization conditions was carried out with Hampton Crystal Screen, Crystal Screen II, Ammonium Sulfate Screen and PEG 6000 Screen and DeCode Genetics Wizard I and Wizard II screens using the sitting-drop vapor-diffusion method. Drops consisting of 2.0 µl purified Nod1_CARD (13.0 mg ml^{-1}) in 10 m*M* sodium phosphate pH 6.0, 130 m*M* NaCl, 1 m*M* DTT and 2.0 µl precipitant solution were equilibrated against 0.9 ml precipitant solution at 277 K. The precipitant solution was diluted by mixing 0.6 ml of the original solution from the kits with 0.3 ml deionized water before use. Small crystals appeared in 20%(*w*/*v*) PEG 6000, 67 m*M* MES pH 6.0. The conditions were optimized using Hampton Additive Screen and StockOptions Salt. Larger crystals were obtained within a month in 20%(*w*/*v*) PEG 6000, 70 m*M* MES pH 6.0, 100 m*M* diammonium hydrogen citrate, 90 m*M* NaI, 1 m*M* DTT. These crystals were still of small size, but X-ray diffraction was observed. In order to produce larger and better diffraction-quality crystals, microcrystals were seeded into new drops containing the same precipitant solution and an equal volume of protein. Crystals appeared within two weeks and reached their maximum dimensions within a month at 277 K (Fig. 1). Crystals were soaked in 20%(*w*/*v*) PEG 6000, 70 m*M* MES pH 6.0, 100 m*M* diammonium hydrogen citrate, 1 m*M* DTT, 20%(*v*/*v*) glycerol for 1 h at 277 K and then in the same solution but with a higher [25%(*v*/*v*)] glycerol content for 3 min prior to flash-cooling in liquid nitrogen.

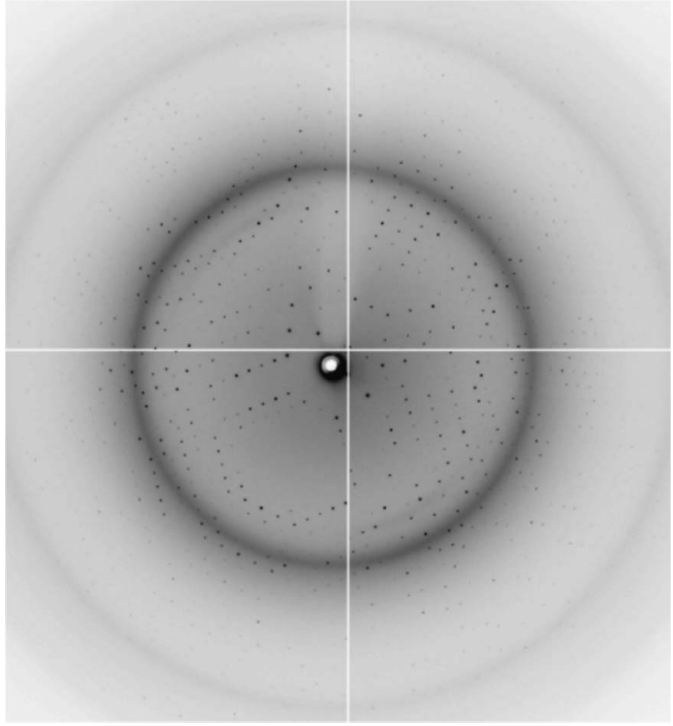

Figure 2
Diffraction image of the Nod1_CARD crystal used for data collection.

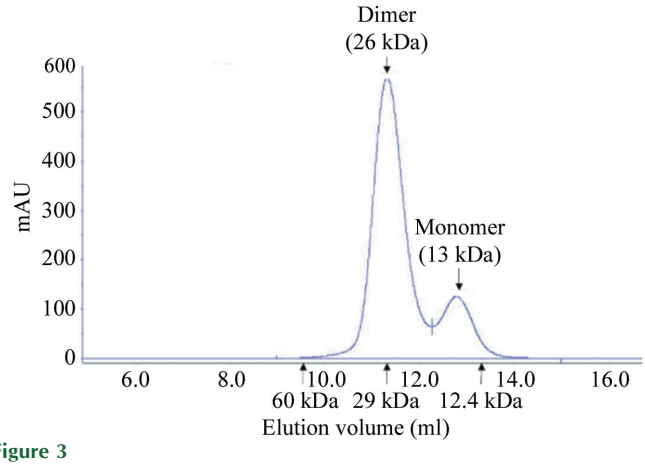

Figure 3
Gel-filtration profile of the Nod1_CARD on Superdex-75. The positions of molecular-weight standards are given at the bottom.

2.3. X-ray data collection and X-ray analysis

X-ray diffraction data were collected to 1.9 Å at 100 K on beamline F2 at MacCHESS (Fig. 2). The data were processed with the *HKL*-2000 program suite (Otwinowski & Minor, 1997). The native crystals belong to space group $P3_1$ or $P3_2$, with unit-cell parameters $a = b = 79.1$, $c = 80.9$ Å. Data-processing statistics are outlined in Table 1.

3. Results and discussion

Gel-filtration experiments showed that Nod1_CARD underwent concentration-dependent dimerization, with a mainly dimeric conformation at the concentration used for crystallization (Fig. 3). Solvent-content analysis showed that the volume of the asymmetric unit of the crystal was compatible with one molecule of dimeric Nod1_CARD. The corresponding Matthews coefficient was 2.81 $Å^3\ Da^{-1}$, with 56.2% solvent content. Extensive molecular-replacement attempts to solve the structure of Nod1_CARD using the crystal structures of the CARDs of Apaf-1 (PDB code 1cy5; Vaughn *et al.*, 1999), caspase-9 (PDB code 3ygs; Qin *et al.*, 1999) and the NMR structure of ICEBERG (PDB code 1dgn; Humke *et al.*, 2000), all of which have a similar death-domain fold, failed owing to low sequence identity. During the preparation of this manuscript, an NMR structure of monomeric Nod1_CARD was reported (PDB code 2b1w; Manon *et al.*, 2007). However, MR trials using this model were also unsuccessful. A search for heavy-atom derivatives to solve the structure by MIR phasing is in progress.

This work was supported in part by the Crohn's and Colitis Foundation of the USA. YCP is a Principal Investigator Fellow of the Cancer Research Institute.

References

Chou, J. J., Matsuo, H., Duan, H. & Wagner, G. (1998). *Cell*, **94**, 171–180.
Girardin, S. E., Boneca, I. G., Carneiro, L. A., Antignac, A., Jehanno, M., Viala, J., Tedin, K., Taha, M. K., Labigne, A., Zahringer, U., Coyle, A. J., DiStefano, P. S., Bertin, J., Sansonetti, P. J. & Philpott, D. J. (2003). *Science*, **300**, 1584–1587.
Humke, E. W., Shriver, K., Starovasnik, M. A., Fairbrother, W. J. & Dixit, V. M. (2000). *Cell*, **103**, 99–111.
Hysi, P., Kabesch, M., Moffatt, M. F., Schedel, M., Carr, D., Zhang, Y., Boardman, B., von Mutius, E., Weiland, S. K., Leupold, W., Fritzsch, C., Klopp, N., Musk, A. W., James, A., Nunez, G., Inohara, N. & Cookson, W. O. (2005). *Hum. Mol. Genet.* **14**, 935–941.
Inohara, N., Koseki, T., Lin, J., del Peso, L., Lucas, P. C., Chen, F. F., Ogura, Y. & Nunez, G. (2000). *J. Biol. Chem.* **275**, 27823–27831.
McGovern, D. P., Hysi, P., Ahmad, T., van Heel, D. A., Moffatt, M. F., Carey, A., Cookson, W. O. & Jewell, D. P. (2005). *Hum. Mol. Genet.* **14**, 1245–1250.
Manon, F., Favier, A., Nunez, G., Simorre, J. P. & Cusack, S. (2007). *J. Mol. Biol.* **365**, 160–174.
Otwinowski, Z. & Minor, W. (1997). *Methods Enzymol.* **276**, 307–326.
Qin, H., Srinivasula, S. M., Wu, G., Fernandes-Alnemri, T., Alnemri, E. S. & Shi, Y. (1999). *Nature (London)*, **399**, 549–557.
Vaughn, D. E., Rodriguez, J., Lazebnik, Y. & Joshua-Tor, L. (1999). *J. Mol. Biol.* **293**, 439–447.
Viala, J., Chaput, C., Boneca, I. G., Cardona, A., Girardin, S. E., Moran, A. P., Athman, R., Memet, S., Huerre, M. R., Coyle, A. J., DiStefano, P. S., Sansonetti, P. J., Labigne, A., Bertin, J., Philpott, D. J. & Ferrero, R. L. (2004). *Nature Immunol.* **5**, 1166–1174.
Weber, C. H. & Vincenz, C. (2001). *Trends Biochem. Sci.* **26**, 475–481.
Yoo, N. J., Park, W. S., Kim, S. Y., Reed, J. C., Son, S. G., Lee, J. Y. & Lee, S. H. (2002). *Biochem. Biophys. Res. Commun.* **299**, 652–658.